Mem. S.A.It. Vol. 7, 198

Memorie della
Supplementi

Spectroscopy of the discharges created and maintained by a surface-wave

M. D. Calzada

Grupo de Espectroscopía de Plasmas, Dpto. de Física, Edificio C-2, Campus de Rabanales. Universidad de Córdoba, 14071 Córdoba, Spain.

Abstract. The discharges created and maintained by a surface-wave are being used in an increasing number of applications in different fields of science and technology. Knowing the processes which take place in the plasma is essential if we want that these applications being done correctly. These processes are related with the characteristic parameters of plasma such as temperatures and densities. For that, it is necessary to measure them. Different methods can be used with this purpose. Among them, the methods of passive spectroscopy do not disturb the discharge because they utilise the intensities and the broadenings of the spectral lines emitted by the plasma. In this work, the methods to measure the gas and electron temperatures, the electron density and the metastable and resonant atom populations are described, including the experimental values of the plasma parameters obtained from them.

Key words. Microwave plasma-Spectroscopic diagnosis methods-Plasma parameters-Spectral line broadening

1. Introduction

The discharges created and maintained by a surface-wave (SWD) are of a special type of microwave discharge, characterized by having dimensions higher than the wavelength of the electromagnetic field that is maintaining them, and the coupler device of the microwave energy. From an experimental point of view, the surface wave discharge has several characteristics that make it especially useful in the research of basic plasma physics, and can also be applied in different fields of science and technology. These characteristics are: a) the wide range of pressure (mTorr-some atmospheres) and frequency (MHz-GHz), b) the use of different atomic (Ar, He, Kr, Xe) and molecular (N_2 and O_2) gases and their mixtures, with flows lower than 0.5 l/min against several l/min that another plasma type such as the ICP needs (~ 10 l/min), c) the discharge extension outside the exciter device and, in this way, long plasma columns, and d) also, to point out, the absence of the significant fluctuations and instabilities and a very good reproducibility.

In recent years, SWDs are used in an increasing number of applications such as surface treatment (formation and deposition of thin material films, in the manufacturing of, for example, electronic devices), light sources, emission of laser radiation, sterilization and spectrochemical analyses (Stafford et al. 2002; Hubert & Sing 1998; Kudela et al. 1998; Calzada et al. 2002). Knowing the processes (internal kinetics) which take place in the plasma is essential if we want correctly to carry out these applications. The processes in the plasma depend on the parameter values of the discharge such as temperatures and densities. The electron density (n_e) is one of the most important parameter. Knowing its value is basic if we want to understand the kinetics of the discharge because the electrons transfer the energy from the microwave field to the plasma, through their collisions with the rest of the particles which constitute it.

Metastable atoms play an important role in the microscopic mechanisms (internal kinetics) that take place in the plasma due to their high energy and their long mean life. They constitute a reserve of chemical energy which can produce endothermic reactions of excitation, ionization and dissociation of the other atoms and molecules. Depending on the discharge conditions, the contribution to the ionization from the metastable levels to the total ionization rate may be very important, influencing the population distributions of the excited states of the plasma atoms (and, therefore, the degree of thermodynamic equilibrium). Besides, the stepwise ionization from them permits a decrease in the necessary energy to sustain the discharge.

On the other hand, the possibility of the different processes (excitation and ionization) in the plasma being carried out will depend on the energy available in the discharge, fundamentally in the form of the kinetic energy of the electrons (electron temperature, T_e) and the heavy particles such as atoms and ions (gas temperature, T_g).

For measuring these parameters we can use techniques of passive spectroscopy, because the wide range and intensity of the spectral lines emitted by the atoms and ions into the discharge. Starting from intensities and broadenings of the spectral lines we obtain information about the basic parameters of the plasma named above.

2. Broadening effects on a spectral line

The shape and width of the spectral lines emitted by the plasma are governed by the processes which happen in the plasma perturbing the emitting atoms and molecules. Moreover, the optical device used in the laboratory to register the lines introduces additional broadening on their profile. The width of the lines is measured at half-way of the height (full width at half maximum, FWHM), and it is represented by $\Delta\lambda$ in the case where de profile of the line is given as a function of the wavelength. The different causes which contribute to the line broadening are briefly described below.

Natural broadening is due to the fact that each quantic state of an atom is not perfectly defined but presents a dispersion of energy because of the perturbations exercise by the electromagnetic fields of the photons on the atom, with an intensity distribution fitting a Lorentz profile (Mitchell & Zemansky 1971).

Doppler broadening is caused by the movement or the thermal agitation of the emitting particles. The velocity distribution of these particles originates a distribution of frequencies due to the Doppler effect, giving rise to a Gaussian type profile. When the particle velocity distribution is Maxwellian, this broadening $\Delta\lambda_D$ depends on the translational (kinetic) temperature (T_g) of the particles originating it (Mitchell & Zemansky 1971).

Collisional broadening (Stark, pressure and resonant) has its origin in the interactions of the emitting particles with the plasma particles. These interactions cause a random perturbation in the energy of the states of the particle emitting the radiation, which produces a broadening of the corresponding emission line. The collisional broadening may be due to various causes independent of each other. On one hand, the *Stark broadening* ($\Delta\lambda_S$), originated by the long range interaction with the charged particles of the plasma (electrons and ions), has a value which basically depends on the value of the electron density and temperature (Griem 1974; Konjević 1999). On the other hand, the so-called *pressure* or *van der Waals broadening* ($\Delta\lambda_W$) is due to the interaction of the excited atoms with the dipole induced in the neutral perturbers and depends on the value of the discharge gas temperature (Konjević 1999); this broadening is larger for spectral lines proceeding from the more external levels, which correspond to higher value of the effective quantum number of those levels (n^*) (Griem 1974); this quantum number is equal to $Z(E_H/E_p)^{1/2}$, where Z is the core charge, E_H is the Rydberg constant or hydrogen ionization energy and E_p is the ionization energy of this level. Finally the so-called resonant broadening ($\Delta\lambda_R$) is a special case in which the perturbers are excited neutral atoms of the same species connected with the ground state (Konjević 1999). Each of these collisional broadenings gives rise to a Lorentz type profile (Mitchell & Zemansky 1971).

Broadening from self-absorption is due to the absorption of the radiation emitted by an atom by another of the same species present in the plasma. The self-absorption process reduces the spectral line intensity, basically in the central part of the profile, which leads to an effective broadening of it being the halfwidth of the self-absorbed line greater than in the case in which there is no self-absorption (Konjević 1999; Christova 2004; Cowan & Dieke 1948).

Instrumental broadening ($\Delta\lambda_I$) is caused by the measuring optical device and being added to the broadening mechanisms related to the processes in the discharge atoms. In many cases the instrumental profile can be approximated to a Gaussian profile without committing any important error.

The profile of the spectral lines in plasmas generated at pressures higher than 100 Torr can be approached by using a Voigt function, characterized by its broadening as $\Delta\lambda_V$. This function type is the result of the convolution of a Gaussian function with a Lorentzian function, their broadenings being $\Delta\lambda_G$ and $\Delta\lambda_L$, respectively. Under this pressure condition (> 100Torr), some broadenings can be neglected and consequently, the Gaussian part of the profile is due to two Gaussian broadenings, the Doppler ($\Delta\lambda_D$) and the instrumental ($\Delta\lambda_I$) ones; the Lorenztzian part to the Stark ($\Delta\lambda_S$) and de van der Waals ($\Delta\lambda_W$) ones. All these broadenings are connected through the following expressions:

$$\Delta\lambda_L = \Delta\lambda_S + \Delta\lambda_W \quad (1)$$

$$\Delta\lambda_G^2 = \Delta\lambda_D^2 + \Delta\lambda_I^2 \quad (2)$$

To unfold the Voigt profile into its Lorentzian and Gaussian components it should be used an adequate software.

3. Experimental device

In this section a schematic description of the plasma source and the optical detection and data acquisition systems for emission spectroscopy measurements is presented in Fig. 1.

The discharge was created in a quartz tube with one of its end open to the atmosphere, obtaining a plasma column. The dimensions of the discharge tube inner and outer diameter were 1-1.5 and 4-8 mm, respectively. The value of the inner diameter was chosen so that the plasma occupied almost the whole cross section of the discharge tube and, in this way, avoids the effect of radial contraction that appears in plasmas generated at a pressure higher than 10 Torr. In the case of microwave discharges, different from DC discharges, the plasma filament can be broken into two o more filaments depending on the operative conditions; among these conditions the radius of the discharge tube is (Kabouzi et al. 2002).

The microwave power for the creation and maintenance of the plasma was between 100 and 250 W and was provided by a SAIREM generator GMP 12 kT/t in continuous mode at a frequency of 2.45 GHz. This power was supplied to the plasma by different exciter devices such as a *surfaguide* (Moisan et al. 1998) and a *surfatron* (Moisan et al. 1976). A stub system was also provided in order to adjust the impedance and ensure that the reflected power was less than 5% of the incident power.

The plasma gas was argon with a purity of about 99.99% at a flux of 0.25 l/min measured by a mass-flow controller.

The optical system consisted of two Czerny Turner monchromators, one of them with a focal length of 1 m and equipped with a holographic diffraction grating of 1200 grooves/mm (Jobin-Yvon THR-1000S) and another one with a grating of 2400 grooves/mm (Jobin-Yvon Horiba1000M). The slit widths used were 100 μm for the line spectra and 30 μm for the molecular band spectra. The detectors were two photomultiplier, R636-10 and R212-UH, of company Hamamatsu designed for the interval 180-900 nm. The radiation emitted by the plasma was collected by an optical fiber at different positions along the

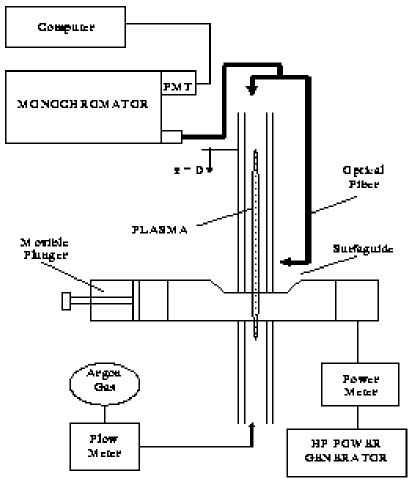

Fig. 1. Schematic diagram of the axially and transversally movable optical fiber that collects light from the plasma

plasma column, z = 0 being the end of the discharge column.

4. Methods to measure the plasma temperatures

4.1. Gas temperature

The gas temperature (T_g) is a measurement of the energy acquired by the heavy plasma particles (atoms and ions) of the discharge, essentially by means of electron collisions. In particular, being responsible for the atomization of the molecules of the substances introduced in the plasma, in order to analyze them. In many cases, the gas temperature is considering equal to the rotational temperature obtained from the ro-vibrational spectra of thermometric molecules present as a trace level in the plasma, assuming that these molecules are in equilibrium with the argon atoms. In this way the rotational temperature is obtained from the slope of the plot of $\lg(I\lambda/A)$ as a function of the transition upper state energy; I is the maximum value of the line intensity and A the corresponding transition probability. The molecules considered with this purpose are namely the OH radicals when, for instance, water vapor is already present as impurity in the carrier gas.

The corresponding axial distribution of the gas temperature obtained from the OH radical spectra is almost constant along the plasma column, with a value between 1200-1500 K. This result has also been reported by several authors under similar experimental conditions (Levésque 1991; Besner 1990; Dobreva et al. 1990). However, in some cases, the OH spectra are too weak. For that, another possibility is to determine T_g from *Doppler* or *Van der Waals broadenings* of the spectral lines emitted by the plasma. The expression that connects the *Doppler* width ($\Delta\lambda_D$) with T_g is given by:

$$\Delta\lambda_D = 7.16 \times 10^{-7} \lambda \sqrt{\frac{T_g}{M}} \tag{3}$$

where T_g is in K, M is the mass of the radiating atom in atomic mass units, and λ is the wavelength in nm. In the case of van der Waals broadening ($\Delta\lambda_W$), the expression is (Ali & Griem 1966; Konjević & Konjević 1997):

$$\Delta\lambda_W = 8.18 \times 10^{-5} \lambda^2 \left(\alpha\langle R^2\rangle\right)^{2/5} \left(\frac{T_g}{\mu}\right) N \tag{4}$$

with N in cm^{-3}, T_g in K and λ in cm. μ is the reduced emitter-perturber mass, α the polarizability in cm^3 and $\langle R^2\rangle$ the mean square radius of the emitting atoms in the upper and lower levels of the transition.

For a value of T_g=1500 K, the *Doppler broadening* varies from 0.0024 nm at 522.1 nm to 0.0033 nm at 737.2 nm. Since $\Delta\lambda_D$ is an order of magnitude lower than $\Delta\lambda_I$ (10^{-2} nm), we can assume that, under experimental conditions, the instrumental broadening dominates the Gaussian component of the recorded profile. For that, it is not possible to measure the gas temperature from the Doppler broadening of the atomic lines. Figure 2 shows that the *Van der Waals broadening* of the 603.2 nm argon line yields an axial variation of the gas temperature with a similar trend to that of the gas temperature inferred from the OH radical. Moreover, the values of T_g determined from both methods are nearly the same.

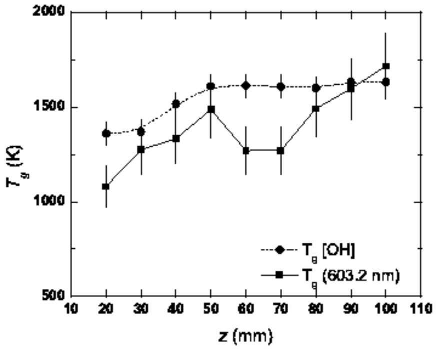

Fig. 2. Axial variation of the gas temperature as observed from an argon line compared to T_g from the OH radical band spectra

4.2. Electron temperature

The energy of the electrons (electron temperature, T_e) is a measurement of a part of the available energy in the discharge, this energy being used in the ionization and excitation processes that take place in the plasma. The electron temperature is one of the plasma parameters more difficult to measure.

The well-known Thomson scattering (i.e. scattering of light by free plasma electrons) can be used for measuring it (Kempkens & Uhlenbush 2000). But, this technique is quite difficult to implement especially in small dimension plasmas. In addition, it requires access to a powerful laser system which makes the method costly. Another possibility is to use methods of passive spectroscopy such as the Boltzmann-plot and the line-continuum ratio methods.

The use of the Bolztamnn-plot method requires assuming that the distribution of population of the top levels obeys the Saha-Boltzmann's distribution, what is to say that the plasma is, at least, in *Partial Local Thermodynamic Equilibrium* (PLTE). This procedure utilizes the (assumed) linear dependence of $\lg(I\lambda/g_pA_p)$, among the atomic levels of the plasma atoms, as a function of the energy (E_{exc}) of the upper level of the transitions. Here, I is the intensity from the total area of spectral line, λ the wavelength, g_p the statistical weight of upper level and A_p the probability of spontaneous emission. This dependence leads to T_e from the slope of the straight line ($-0.625/T_e$). Table 1 lists the lines and their characteristic parameters used in the Boltzmann-plot.

Table 1. List and characteristics of the ArI spectral lines used in the Boltzmann-plot

λ (nm)	E_{exc} (cm^{-1})	g_p	A_p ($10^6 s^{-1}$)	Transition
425.1	166 660	3	0.113	5p-4s
425.9	118 871	1	4.15	5p-4s
426.6	117 184	5	0.333	5p-4s
427.2	117 151	3	0.84	5p-4s
430.0	116 999	5	0.394	5p-4s
433.3	118 469	5	0.60	5p-4s
433.5	118 460	3	0.38	5p-4s
434.5	118 407	3	0.313	5p-4s
518.8	123 373	5	1.38	5d-4s
522.1	124 610	9	0.92	7d-4s
549.6	123 653	9	1.76	6d-4s
555.9	122 087	5	1.48	5d-4s
560.7	121 933	3	2.29	5d-4s
591.2	121 012	3	1.05	4d-4s
603.2	122 036	9	2.46	5d-4s
641.6	119 683	5	1.21	6s-4s
696.5	107 496	3	6.70	4p'-4s
706.7	107 290	5	3.95	4p'-4s
750.4	108 723	1	47.2	4p'-4s'
826.5	107 496	3	16.8	4p'-4s'
842.5	105 617	5	23.30	4p'-4s
866.8	106 037	3	2.80	4p'-4s'

But the Boltzmann-plot-method can not be used in plasmas created with gases such as He or Ne because they are very far from the pLTE. In this case it is necessary to use other methods. An alternative is the line-continuum ratio method that utilises the intensity I emitted and the adjacent continuum ε_c, I/ε_c being a function of T_e. For an argon plasma the used line is 430.01 nm and the expression of the I/ε_c is (Sola et al. 1995):

$$\frac{I}{\varepsilon_c} = \frac{A}{T_e}\exp\left(\frac{B}{T_e}\right)$$

Table 2. Comparation between the $T_e(\pm 15\%)$ values obtained from the Boltzmann-plot and the line-continuum ratio method

Methods	z position (cm)					
	2	4	6	8	10	12
Boltzmann-plot	4300	4800	5500	5800	6300	6800
Line-continuum	4600	5100	5900	6100	6500	7100

$$\times \exp\left(-\frac{C}{T_{exc}}\right)\left[1.8 - 0.7\exp\left(-\frac{D}{T_e}\right)\right] \quad (5)$$

with $A = 255.2$ in nmK, and $B = 182839.7$, $C = 168320.4$ and $D = 33450.1$ in K. In Table 2 the T_e values obtained by both methods, Boltzmann-plot and line-continuum ratio are presented. One observes that the electron temperature increases with z, and this behavior is different to the gas temperature, whose value remains constant along the plasma column. Also the values provided by both methods are very similar and they can be considered equals.

5. Measurement of the electron density

The electron density (n_e) is one of the most important parameter to measure in laboratory plasmas because the electrons control the processes of ionization and excitation that take place in them.

The Stark broadening of the spectral lines is often used as a technique for the diagnosis of the electron density, with applications not only in the laboratory plasmas, but also in the astrophysics. The procedure is based on this broadening, but it depends on the density of charged particles in the sourrounding of the emitter, according to the Stark effect.

The hydrogen Balmer lines such as H_α, H_β and H_γ are classically utilized by this purpose. However, under certain experimental conditions, these lines are not intense enough, and it is necessary to introduce small quantities of hydrogen into the plasma as water vapour. This introduction, even very slight ($\sim 1\%$), produces changes in the internal kinetics of the discharge. A straightforward solution to this problem is to determine n_e from the Stark broadening of spectral lines emitted by the discharge gas itself.

5.1. Stark broadening of the Balmer series

Stark broadening of the Balmer lines is the most popular approach to the determination of n_e, since the broadening of hydrogen lines is the strongest: these lines are thus the most sensitive to electron density variations. The classical expression connecting the Stark width with n_e has been derived by Kepple & Griem (1968) theory (*KG theory*), who did not take into account the influence of the ion dynamics on the spectral profiles of the Balmer lines. This expression is written as:

$$\Delta\lambda_S = 2.50 \times 10^{-10} \alpha_{n'n}(n_e T_e) n_e^{2/3} \quad (6)$$

where $\Delta\lambda_S$ is in nm. The electron density is expressed in cm^{-3} and the parameter $\alpha_{n'n}(n_e T_e)$ is tabulated for each element, each transition $n'n$ and different values of T_e and n_e (Griem 1974). According with this theory, the theoretical profiles of the Balmer lines of the hydrogen have a different structure respect to the ones of the experimental profiles. In this way, the discrepancy between the theoretical and experimental profiles is normally adscribed to the ion dynamics effect, which must not be neglected if we have a plasma with a low electron density.

To introduce an important effect such as the ion dynamics on the line profiles several mod-

Table 3. Values of electron density obtained from the hydrogen Balmer lines and using the *KG theory* (without ion dynamics) and the *GC model* (whit ion dynamics)

Lines	$n_e(10^{14}\mathrm{cm}^{-3})$	
	KG theory	*GC model*
H_α	13 ± 2	2.8 ± 0.5
H_β	3.3 ± 0.7	2.8 ± 0.2
H_γ	4.9 ± 0.3	2.9 ± 0.2

els have been proposed. Gigosos & Cardeñoso (1996) have developed a computational model (*GC model*) to describe the line profiles including this effect on them. From their computational model, they have obtained a series of tables that provide the Stark broadening ($\Delta\lambda_S$) of the line profile depending on the electron density, electron temperature and the reduced mass (μ) of the pair emitter-ion. The use of this model provides the same electron density value from the different Balmer lines.

Table 3 shows the electron density values obtained from H_α, H_β and H_γ lines using the *KG theory* (without ion dynamics) and the *GC model* (with ion dynamics). This shows that the profile of H_α line is much more greatly influenced by the ion dynamics than the H_β line. So, from Eq. (6) the electron density is overestimated by a factor of 10 in the case of H_α with respect to the value obtained when the *GC model* is used. The H_β line is almost insensitive to the effect of the ion dynamics, as can be observed when comparing both procedures and this has allowed to use it, until now, as an effective tool for the diagnostics of the electron density.

Our results for H_α and H_β lines have been compared to the ones obtained experimentally by Ehrich & Kelleher (1980) and Weber et al. (1983) (Figs. 3a and 3b). In these figures, the continuous line corresponds to the theoretical values obtained from Eq. (6), and the discontinuous line to extrapolated values

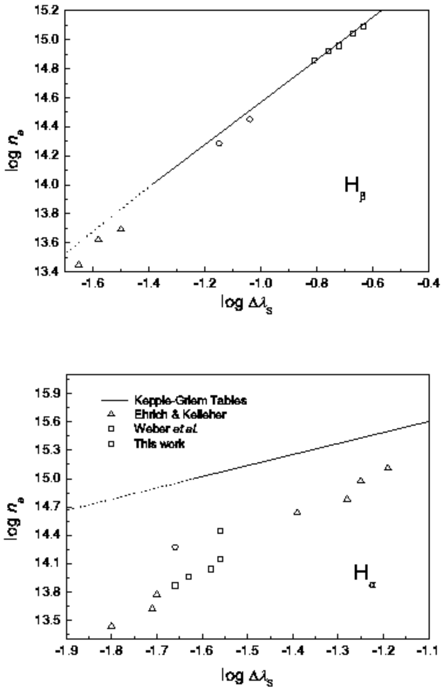

Fig. 3. Comparison of our n_e values from a) H_β and b) H_α with those obtained by other authors

of this expression for densities in the interval $10^{13} - 10^{14}\mathrm{cm}^{-3}$.

In Fig.3a (line H_β) one can see that our values follow Eq. (6) and shows the same tendency as other author values. Besides this, the deviation of the obtained values of n_e taking into account, or not, the effect of ion dynamics on the profiles is very small. Only in the interval $10^{13} - 10^{14}\mathrm{cm}^{-3}$ there is a slight difference which can be mainly attributed to the effect of ion dynamics at these densities.

The experimental values of n_e obtained from H_α line (Fig. 3b) are very different to those obtained with *KG theory*, even at densities of $10^{15}\mathrm{cm}^{-3}$, which proves that ion dynamics strongly affect the profile of this line. These results show that the use of the *GC model* improves the overestimation of the density that results when Eq. (6) is used, principally in the case of the H_α line.

5.2. Stark broadening of neutral atom lines

For the atomic lines, the quadratic Stark effect results in a FWHM which can be expressed by the following classical relationship (Griem 1974; Pellerin et al. 1996):

$$\Delta\lambda_s = 2w[1 + 1.75\alpha(1 - 0.75r)], \qquad (7)$$

where w is the half width at half-maximum due to the collisions with the electrons, α represents the broadening due to the ions and r is the ratio of the mean distance between ions to the Debye length. There are certain restrictions applying to Eq. (7), namely $\alpha \leq 0.5$ and $r \leq 0.8$.

Recently we have made a study of the lorentzian broadening of the ArI spectral lines in order to use their Stark broadening to measure the electron density and not this broadening for Balmer lines. Figure 4 shows the axial variation of the lorentzian component ($\Delta\lambda_L$) of the profile for argon lines belonging to the nd-4p transitions ($4 \leq n \leq 7$). We observe that the total Lorentzian width, resulting from Stark and Van der Waals broadenings, increases with the excitation energy of the upper level of the transition, which corresponds to an increase of the effective quantum number (n^*).

In a surface-wave plasma of Ar the electron density shows an axial distribution which decreases towards the end of the plasma column. For spectral lines corresponding to n^* higher than 5 (522.1 and 549.6 nm), the lorentzian width varies significantly along the plasma column as shown in Fig.4. This increase corresponds to an increase in the electron density along the axis since the gas temperature being axially almost constant requires the Van der Waals broadening to be constant. The observed substantial increase in the line broadening reflects the sensitivity of these lines to electron density variation.

Figure 5 shows the axial distribution of n_e determined from both the broadening of the 549.6 nm argon line and H_β line for comparison. We observe that the variation of electron density, from both lines, with z is similar. However, the actual values stemming from the Ar line is approximately 1.5 or 1.8 times higher than those obtained from the H_β line. The observed difference could be due to the uncertainties of the semi-empirical values of w and α given by Eq. (7) for the 549.6 nm line.

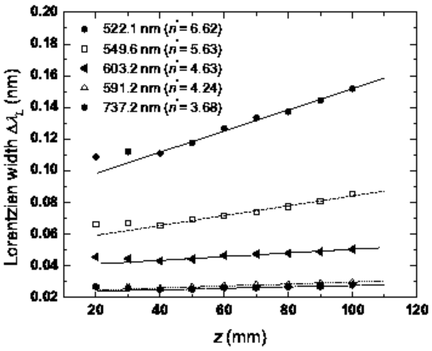

Fig. 4. Axial variation of the width of the Lorentzian component of the observed profile of several argon lines (nd-4p transitions)

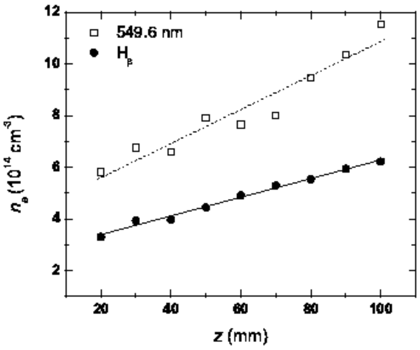

Fig. 5. Comparison of n_e values obtained from both H_β line and 549.6 nm Ar line

6. Populations of metastable atoms

Absorption methods have been used to measure the population of the metastable and resonant levels in discharges (Mitchell & Zemansky 1971; Moussounda et al. 1985; Jolly & Tozeau 1975). These methods are based on the interaction between the radiation and the absorbing atoms, described by

(Mitchell & Zemansky 1971). In this way, a fraction of the radiation emitted by an external source of light is mainly absorbed by the metastable and resonant atoms and this absorbed radiation is related to their densities. However, an external source is not needed when the self-absorption techniques are used with this purpose. These techniques employ the discharge as source of radiation and an absorbing medium (Jolly & Tozeau 1975). Then, the light emitted from the discharge has to travel through the interior of the plasma before coming out to outside. During this passage, part of the radiation is being absorbed by the atoms or molecules of the same kind that causes the emission (Sola et al. 1995). This absorption phenomenon in the light source itself is called *self-absorption*.

In the *self-absorption method*, the ratio of the total intensities of two partially self-absorbed lines emitted by the discharge is used. Both lines end in the same level whose population is aimed to determine: line (1), whith the highest oscillator strength, will be more strongly absorbed than line (2). If we measure the total intensities emitted by these lines in the absence of absorption , I_{01} and I_{02}, and the total self-absorbed intensities, I_1 and I_2, the ratio of these amounts, which depends on the population of the absorbing level, will be written as follows:

$$r = \frac{I_1}{I_2} / \frac{I_{01}}{I_{02}} = r\left(k_{01} l, \frac{k_{01}}{k_{02}}, a_1, a_2\right), \tag{8}$$

where k_0 has the expression:

$$k_0 = \frac{2e^2}{mc} \sqrt{\pi \ln 2} \frac{Nf}{\Delta\nu_D}, \tag{9}$$

f being the oscillator strength of the spectral line and N the absorbing atoms concentrations (metastables or resonants) and the *a-parameter* is the ratio of the Lorentzian and Doppler widths at half-height of the line and it can be expressed in wavelength units as $a = \Delta\lambda_L \sqrt{\ln(2)}/\Delta\lambda_D$.

The line-set used in the measurement of metastable and resonant atom populations is shown in Table 4, as well as both their characteristic parameters and the *a-parameter* values.

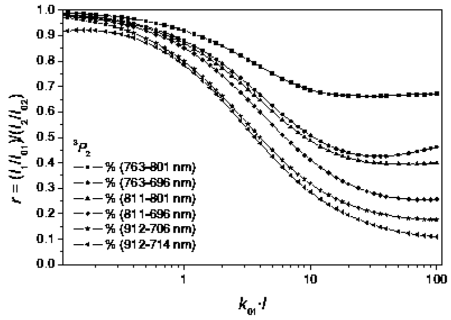

Fig. 6. Ratio r of intensities as function of the absorption parameter for different pairs of spectral lines

For the *a-parameter*, we used the expression in function of wavelength; in this way $\Delta\lambda_L$ has been determined through the deconvolution of the experimental lines, by using a computational program, and $\Delta\lambda_D$ from the discharge gas temperature value.

In Fig. 6, one shows the variation of r as a function of $k_{01}l$, for different values of k_{01}/k_{02}, a_1 and a_2 corresponding to each line pair used in $^3P_2$ metastable level population measurement. These curves have been designed using the tables given by Jansson & Korb (1968), who resolved the Voigt integral using the Romberg's algorithm. Similar curves can be obtained for the lines ending on the $^3P_0$, $^1P_1$ and $^3P_1$ levels.

Figure 7 shows the population of the metastable and resonant argon levels obtained from the intensity ratio of the different line pairs, using the *a-parameter* values experimentally found for them and the r vs. $k_{01}l$ curves previously described Santiago et al. (2004). The results obtained are between 10^{10} and $10^{12}\mathrm{cm}^{-3}$ in agreement with the ones reported in the literature (Moussounda et al. 1985), the $^3P_2$ metastable level being the most populated one. The differences observed among the population values obtained for a same level by using different line pairs are in the error range of the method (20%). This error can be mainly ascribed to the uncertainly in the measurement of the gas temperature, which determined the Doppler broadening that appears in

Table 4. Parameters of the pair lines corresponding to transitions 4p → 4s used to measure the metastable and resonant atom populations

λ(nm)	Transition	E_{exc}(eV)	f	a	g_p	$A_p(10^7 s^{-1})$
811.5	$4p(^3D_3)$-$4s(^3P_2)$	13.0719	0.51	0.54	7	3.66
801.5	$4p(^3D_2)$-$4s(^3P_2)$	13.0910	0.092	0.51	5	0.96
763.5	$4p(^1D_2)$-$4s(^3P_2)$	13.1680	0.239	0.56	5	2.74
714.7	$4p(^3P_2)$-$4s(^3P_2)$	13.2788	0.00299	0.00	3	0.065
706.7	$4p(^3P_0)$-$4s(^3P_2)$	13.2984	0.0296	0.97	5	0.395
696.5	$4p(^3P_1)$-$4s(^3P_2)$	13.3239	0.0292	0.20	3	0.67
842.5	$4p(^3D_2)$-$4s(^3P_1)$	13.0910	0.413	1.21	5	2.33
810.4	$4p(^3D_1)$-$4s(^3P_1)$	13.1493	0.273	0.74	3	2.77
800.6	$4p(^1D_2)$-$4s(^3P_1)$	13.1680	0.075	0.91	5	0.468
751.5	$4p(^1P_1)$-$4s(^3P_1)$	13.6910	0.121	1.04	1	4.3
866.8	$4p(^3D_1)$-$4s(^3P_0)$	13.1493	0.095	1.44	3	0.28
794.8	$4p(^3P_2)$-$4s(^3P_1)$	13.2788	0.56	0.36	3	1.96
852.1	$4p(^3P_2)$-$4s(^1P_1)$	13.2788	0.160	6.20	3	1.47
840.8	$4p(^3P_0)$-$4s(^1P_1)$	13.2984	0.431	6.06	5	2.44
826.5	$4p(^3P_1)$-$4s(^1P_1)$	13.3239	0.172	6.11	3	1.68
750.4	$4p(^1S_0)$-$4s(^1P_1)$	13.4760	0.133	5.26	1	4.72

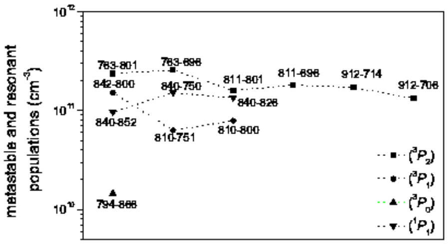

Fig. 7. Metastable and resonant argon populations measured by using different pairs of spectral lines

the expression of *a-parameter* and in the expression used in the calculation of the absorbing atoms (Eq.(9)).

Acknowledgements. The research presented in these pages has been possible thanks to the work of the components of the *Grupo de Espectroscopía de Plasmas* from the University of Córdoba (Spain): M. Carmen García (Dr.), Manuel Sáez (Dr.), Isabel Santiago (Dr.), Abel Sáinz (Ph.D Student), Cristina Yubero (Ph.D Student), Juana Martínez (Ph.D Student), Manuel Pineda (M.Sc. Student), José Muñoz (M.Sc. Student) and Margarita Jiménez (M.Sc. Student). Also, the author thanks to the professor Michel Moisan (Université de Montréal, Québec, Canada) his support and help during the formation step of the research group. This work has been partially supported by the *Vicerrector Office of Scientific Policy* of the Córdoba University, the project No. FTN2002-02595 of the Ministerio de Ciencia y Tecnología (Spain) and the European Community (FEDER founds),

References

Ali, A. & Griem, H. R. 1966, Phys. Rev. A, 144, 366

Besner, A. 1990, PhD. Thesis, Université de Montréal, Québec, Canada

Calzada, M. D. et al. 1996, J. Appl. Phys., 80, 46

Calzada, M. D. et al. 2002, J. Appl. Phys, 92, 2269

Christova, M. 2004, Appl. Spectrosc., 58, 1032
Cowan, R. D. & Dieke, G. H 1948, Rev. Modern Phys., 20, 418
Delcroix, J. L. et al. 1975, *Atomes et molecules metastables dans le gaz ionisé*, CNRS
Dobreva, V. et al. 1990, 22^{nd} EGAS, Vol. II, P3-91, 754
Ehrich, H. & Kelleher, D. E. 1980, Phys. Rev. A, 319
García, M. C. et al. 2000, Spectrochim. Acta B, 55, 1733
Gigososo, M. A. & Cardeñoso, V. 1996, J. Phys. B, 29, 4795
Griem, H. R. 1974, Spectral line broadening by plasmas, Academic, New York
Hubert, J. & Sing, R. 1998, J. Phys IV France, 8, 357
Jansson, P. A. & Korb, C. L. 1968, JQRST, 8, 1399
Jolly, J. & Tozeau, M. 1975, JQRST, 15, 863
Kabouzi, Y. et al. 2002, J. Appl. Phys., 91, 1008
Kempkens, H. & Uhlenbush, J. 2000, Plasma Source Sci. Technol., 9, 492
Kepple, P. & Griem, H. R. 1968, Phys. Rev., 173, 317
Konjević, N. 1999, Phys. Rep., 316, 339
Konjević, R. & Konjević, N. 1948, Spectrochim. Acta B, 52, 2077
Kudela, J. et al 1998, Jpn. J. Appl. Phys., 37, 4169
Levésque, S. 1991, M. Sc. Thesis, Université de Montréal, Québec, Canada
Mitchell, A. C. G. & Zemansky, M. W. 1971, *Resonance Radiation and Excited Atoms*, Cambridge
Moisan, M., Etemadi, E., & Rostaing, J. C., 1998, *European Patent Specification*, EP 0874 537 A1
Moisan, M. et al. 1976, *Perfectionnements apportés aux dispositifs d'excitation par des ondes HF, d'une colonne de gaz enfermée dans une enveloppe*, Brevet, France
Moussounda, P. S. et al. 1985, Spectrochim. Acta B, 40, 641
Pellerin, S. et al. 1996, J. Phys. B, 29, 3911
Santiago, I. et al. 2004, Eur. Phys. J. Appl. Phys., 28, 325
Sola, A. et al 1995, J. Phys. D, 28, 1099
Stafford, L. et al 2002, J.Vac. Sci. Technol. A, 20, 530
Weber, E. W. et al. 1983, Appl. Phys. B, 32, 63